Journal of Applied Polymer Science

Influence of Residence Time on Performances of PVDF Membranes Prepared via Free Radical Polymerization

Gui-E Chen,[1] Wen-Zhi Wu,[1] Ping-Yun Zhang,[2] Zhen-Liang Xu[2]

[1]School of Chemical and Environmental Engineering, Shanghai Institute of Technology, Shanghai 201418, China

[2]State Key Laboratory of Chemical Engineering, Membrane Science and Engineering R&D Lab, Chemical Engineering Research Center, East China University of Science and Technology, Shanghai 200237, China

Correspondence to: G.-E. Chen (E-mail: chenguie@sit.edu.cn) or Z.-L. Xu (E-mail: chemxuzl@ecust.edu.cn)

ABSTRACT: Poly(vinylidene fluoride) (PVDF) membranes were prepared with various residence times using water–ethanol (50 : 50, mass ratio) and pure ethanol coagulants as first coagulant, respectively. The physical properties of PVDF solution after free radical polymerization were investigated by dynamic light scattering (DLS), scanning electron microscopy (SEM), viscosity, precipitation kinetics, and surface tension. Resultant PVDF membranes were characterized by SEM, contact angle, mechanical properties, and filtration properties. The results showed that the longer residence time in the first coagulant contributed to the filtration properties improvement. Contact angles of the top-surfaces and bottom-surfaces of membranes decreased as residence time increasing in the first coagulant, and the top-surface showed better hydrophilicity than that of the bottom-surface. The pore size distributions of PVDF membranes showed that the dominating demixing process of the casting solution in water–ethanol coagulant was 5 s, and in that of ethanol was 10–15 s. Additionally, the short-time delay demixing process in water–ethanol first coagulant resulted in a thin dense layer near the top surface, and the longer time delay demixing process in that of ethanol contributed to the shift of the inter-globules to the cellular morphology in the case of the residence time increasing. © 2013 Wiley Periodicals, Inc. J. Appl. Polym. Sci. **2014**, *131*, 39987.

KEYWORDS: membranes; separation techniques; free radical polymerization

Received 11 April 2013; accepted 20 September 2013

DOI: 10.1002/app.39987

INTRODUCTION

Membrane has been broadly used in many fields, such as wastewater treatment,[1–3] food processing industry,[4–8] petrochemical industry,[9,10] and bio-separation.[4] PVDF is one of the most popular materials for membrane preparation due to its excellent chemical resistance, good thermal stability, and mechanical properties.[11–14] PVDF membranes are mainly fabricated via NIPS process, which is immersing the casting solutions into a non-solvent coagulation bath to induce phase separation, first the diffusive exchange between solvent and non-solvent introduces the liquid–liquid demixing process, and then the successive liquid–solid phase separation produces a porous structure.[15–17] According to the bimodal demixing membrane formation mechanism, the nucleation and growth of PVDF starts from the lean phase, subsequently, the solidification of PVDF rich phase, or the crystallization of PVDF phases fix the membrane morphology.

The functions of PVDF membranes are greatly influenced by their physical morphology and chemical composition. The hydrophobic nature of PVDF makes it easily susceptible to fouling and permeability decline, which affects their application in water purification from diverse sources, such as seawater, produced water, industrial wastewater, and other polluted water sources.[18–20] Optimized structures of PVDF in terms of the membrane surface properties, structures, and mechanical properties are anticipated for various applications in the areas of purification and separation. Precise modulation of the high-performance membranes with high hydrophilicity, high selectivity and fluxes, excellent mechanical properties, low fouling tendency, and defect-free production could yield effective oil-aqueous suspension solution systems. A large number of methods for improving the hydrophilicity and the antifouling property of PVDF membranes have been researched.[21–26] Blending is a widely applied method in the modification of the polymeric porous membrane as it can modified not only the membrane surface, but also the pore channels.[27] Normally, the hydrophilic blending additives such as polyvinyl pyrrolidone (PVP)[28–31] or polyethylene glycol (PEG)[32–36] are used to modify PVDF as they are water soluble and easily lost during the

Additional Supporting Information may be found in the online version of this article.

membrane preparation and operation processes. However, the main role of these additives in the preparation process of PVDF membrane process is the pore-forming agents, not the modifier. In recent years, the blending of the self-synthesized amphiphilic copolymers as the antifouling surface modifiers, pore-forming additives, and tune membrane morphology has received much attention in the surface modification of PVDF membranes.[37–39] The amphiphilic copolymers are special molecules with both the hydrophobic hydrocarbon chains and hydrophilic chains (polar head groups), which tends to form various micelle structures in the polarity solution, and those structures could contribute to the porous structure formation. During demixing process, the hydrophobic chains of the amphiphilic polymer could twine the PVDF bulk and the hydrophilic chains would enrich and segregate on the membrane surface, which contributes to the fouling resistance enhancement of resultant PVDF membranes. Liu et al. blended PVDF powder with the refined amphiphilic brush-like copolymer P(MMA-r-PEGMA) self-synthetized by atom transfer radical polymerization (ATRP) method to prepared hydrophilic and fouling resistant those PVDF hollow fiber membranes.[38] Hashim et al. prepared the hydrophilic flat sheet of PVDF membranes by adding the PVDF polymer powders directly to the amphiphilic copolymer mixture containing PVDF grafted with PEGMA.[40] They focused on the influence of the concentration of the amphiphilic copolymer and the coagulation mixture compositions on membranes performances in terms of the filtration properties morphologies and crystalline structure.[41]

Besides, a good solvent is essential in formulating a uniform polymer solution, and in obtaining the membranes with tunable morphologies and performances. PVDF membranes are systematically prepared using 100 : 0, 70 : 30, 60 : 40, 30 : 70, 0 : 100 (TEP : DMAc, mass ratio) as solvents based on the literature.[42] The formulation of TEP-DMAc (70 : 30, mass ratio) cosolvent was selected after optimization the performances of those resultant PVDF membranes. So in this study, TEP-DMAc (70 : 30, mass ratio) is used as cosolvent to obtain targeting PVDF membrane. We aim to prepare the PVDF flat sheet membranes via polymerization method by directly adding azobisisobutyronitrile (AIBN) into the PVDF-TEP-DMAc-PEGMA-MMA system to initiate the polymerization, as shown in Figure 1. In situ free radical polymerization is an easy and economical method, which provides the morphology modulation of PVDF membranes through tuning the microstructure of polymer solution in the cosolvent (Supporting Information, Tables s1, s2, s3, and s4; Figures s1, s2, s3, s4, and s5). As show in Figure 2, water–ethanol (50 : 50, mass ratio) and ethanol are chosen as the first coagulants, after the casting solution is immersed into the first coagulant with various residence times, then the casting solution is immersed into second coagulant (deionized water). The effect of the various residence times of casting solution in the first coagulants and the compositions of the first coagulants on the membrane configurations and the performances in terms of the filtration properties, hydrophilicity, and mechanical properties are investigated.

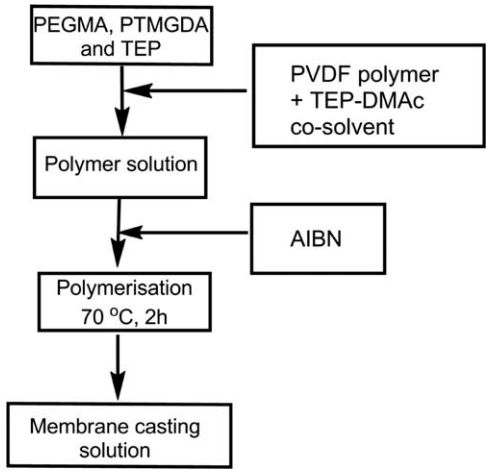

Figure 1. The flow diagram of membrane casting solution preparation process.

EXPERIMENTAL

Materials

Poly(vinylidene fluoride) (PVDF, Solef® 6010) was provided by Solvay Advanced Polymers, L.L.C (Alpharetta, GA, USA). *N,N*-dimethylacetamide (DMAc), methyl methacrylate (MMA), basic alumina, ethanol, triethyl phosphate (TEP), and azobisisobutyronitrile (AIBN) were supplied by Shanghai Sinopharm Chemical Reagent. Poly(ethylene glycol) methyl ether methacrylate (PEGMA, M_n = 1200, industrial grade) was the red-brown liquid and purchased from Taijie Chemical (China, Shanghai). AIBN was recrystallized from pure ethanol before use. Bovine serum albumin (BSA) (MW 67K) and Dextran (MW 40K, MW 70K, MW 100K, MW 500K, and MW 2000K) were purchased from Lianguan Biochemical Reagent Company of Shanghai and Sigma-Aldrich, respectively. Deionized water was prepared in our own lab. Other chemicals used for experiments were of analytical grade without further purification.

Preparation of Hydrophilic PVDF Membranes

PEGMA (120.0 g, 0.1 mol), MMA (6.6 g, 0.06 mol), and TEP (70.6 g) mixture was purified by 4.0 wt % basic Al_2O_3, then the mixture was charged into a conical flask with plug and kept in dark place for further use. Eighteen grams PVDF polymer, 6.0 g purified mixture of PEGMA, MMA, and TEP mixture and TEP-DMAc cosolvent were mixed at 60°C to ensure complete dissolution of the polymers. When the solution was cooled to ambient temperature, a certain amount of the recrystallized AIBN with 0.06 g ([AIBN]/[MMA + PEGMA + TEP] = 1/100, mass ratio) was added into the corresponding casting solution, and the system was stirred for 4 h for well dispersion of AIBN. Then the reaction system was heated to 70°C and polymerization was performed at 70°C for 2 h, and the standing time of the casting solution was at least 12 h to eliminate the inside bubbles.

The homogeneous PVDF casting solutions at the ambient temperature were cast onto a glass plate at 25°C and 60% relative humidity by means of a glass rod, and then were immediately immersed into the water–ethanol and ethanol coagulants (at 25°C) with various residence times of 5 s, 10 s, 15 s, 30 s, then were immersed into the deionized water. The membranes were

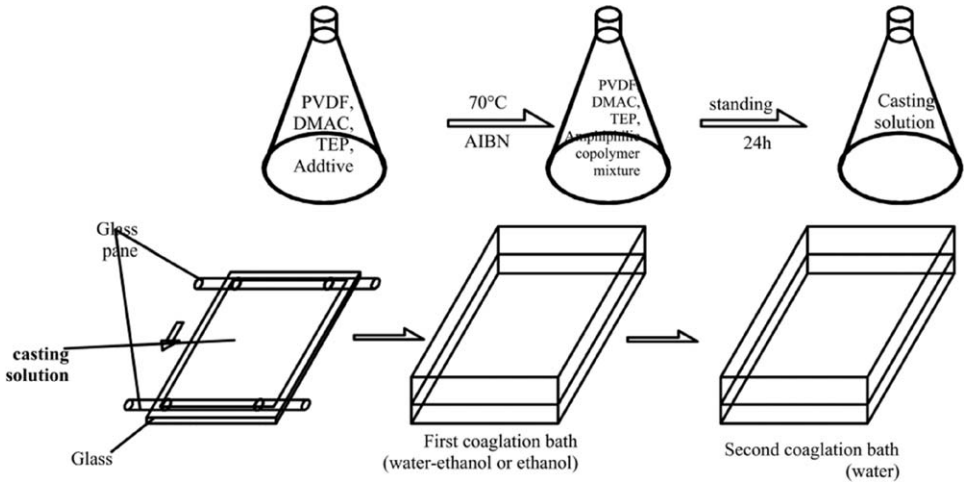

Figure 2. The flow diagram of PVDF flat membrane preparation process.

kept in the fresh water for 1 week, and the deionized water was changed three times a day to ensure completely removal of the residual solvent. The preparation conditions of the membranes were summarized in Table I.

Basic Physical–Chemical Properties of Casting Solution

Viscosity. The viscosity of PVDF casting solution was acquired using a DV-II+PRO Digital Viscometer (Brookfield, USA) at 298 K (controlled by water bath). The reported curves are viscosity versus shear rate curves.

Surface Tension. The surface tension of casting solution was measured by JK99C Automatic Surface and Interface Tension Measure Instrument (Shanghai Zhongcheng Digital Technology Apparatus, China) via the Wilhelmy plate method at ambient temperature.

Conformation of PVDF in Casting Solution Via Free Radical Polymerization. The morphology of dope solution via polymerization was detected by dynamic light scattering (DLS, Zatasizer Nano ZS, Malvern Instruments, U.K.). The conformation of 1.0 wt % PVDF in the TEP-DMAc-PEGMA-MMA system via polymerization was investigated. The DLS method is a simple but precise measurement method to obtain the information about polydispersity of the micelles.[39] The technique measures the time-dependent fluctuations in the intensity of scattered light from a suspension of particles undergoing random, Brownian motion. In DLS, the temporal fluctuations of light scattered by diffusing particles in liquid suspension are measured, which are sensitive to the diffusive motion of the particles. The scattering intensity data were derived by the auto-measure software (Malvern Instruments, Malvern, U.K.) to obtain the harmonic intensity weighted average hydrodynamic diameter (R_h). The mean diameter of the ensemble of particles, also referred to as the *z*-average diameter (D_h) of the reverse micelles, was derived from the slope of the linearized form of the correlation function.

Then the conformation of 18.0 wt % PVDF in TEP-DMAc-PEGMA-MMA system via simplified blend was further validated. The cosolvent of some amount of PVDF casting solutions with various compositions was quickly volatized at 80°C in DHG Series Heating and Drying Oven (Jing Hong Laboratory Instrument, Shanghai), and then the samples were sputtered with gold. The morphology of those casting solution was obtained using scanning electron microscope (SEM, S-3400N, Hitachi).

Characterization of the Precipitation Kinetics of Casting Solutions. The precipitation kinetics of the casting solutions was investigated by dynamic light transmittance experiment, which was carried out by a self-made device as described by Zhang et al.[28] A collimated laser was directed toward the glass plate immersed in water, water–ethanol, and ethanol coagulants. The light intensity was captured by the detector and then recorded on computer.

Membrane Characterization

Filtration Properties of the Resultant PVDF Membranes. Filtration properties of the membranes were characterized by the determination of permeation flux (J), porosity (e), flux recovery ratio (FRR), and pore size distribution. A round-shaped

Table I. esultant PVDF Membranes and Their Corresponding Preparation Conditions

Membrane list	Dope solution composition (wt %, mass ratio) (PVDF/TEP/DMAc/ monomer mixture)	Coagulant	Residue time (s)
MWE-5	18.2/53.3/22.9/6.0	Water–ethanol	5
MWE-10	18.2/53.3/22.9/6.0		10
MWE-15	18.2/53.3/22.9/6.0		15
MWE-30	18.2/53.3/22.9/6.0		30
ME-5	18.2/53.3/22.9/6.0	Pure ethanol	5
ME-10	18.2/53.3/22.9/6.0		10
ME-15	18.2/53.3/22.9/6.0		15
ME-30	18.2/53.3/22.9/6.0		30

WE: water–ethanol (50 : 50, mass ratio) coagulant; E: pure ethanol coagulant.

membrane with constant membrane area (A) 2.289 $\times$ 10^{-3} m^2 was installed into a cell and the pressure in the cell was maintained at 0.1 MPa. Thus, pure water was forced to permeate through the membrane, and the flux was recorded as J_w after compaction of the membranes with stable flux. After that, a 300 mg/L BSA was forced to permeate through the membrane at the same pressure and the flux was recorded as J_B. To confirm the water flux recovery property of these BSA permeated membranes, pure water flux (J_R) was measured after washing them with pure water three times in 0.5 h. The pore size distribution of membranes was characterized by a solute transport of 300 mg/L dextran (MW 40K, MW 70K, MW 100K, MW 500K, and MW 2000K) solution via ultrafiltration experiments; the mean effective pore size (μ), the geometric standard deviation (σ), and MWCO were obtained according to the method described by Yang.[43]

The pure water flux and flux recovery ratio (FRR) was calculated as follows[21,28]:

$$J_w = \frac{V}{A \times t} \quad (1)$$

$$\mathrm{FRR}(\%) = \frac{J_R}{J_w} \quad (2)$$

where J is the flux of membrane for pure water or BSA solution $\{L/(m^2h)\}$, V is the permeate volume of pure water or BSA solution (L), A is the membrane area, and t is the microfiltration time (h).

For all the filtration experiments, the flux measurements were performed thrice and averaged.

Porosity (ε) of resultant membranes was defined by the following equation:

$$\varepsilon(\%) = \frac{(m_1 - m_2)/\rho_G}{(m_1 - m_2)/\rho_G + m_2/\rho_p} \quad (3)$$

where m_1 is the weight of the wet membrane (g), m_2 is the weight of the dry membrane (g), ρ_G is the ethanol density (0.789 g/cm^3), and ρ_P is the polymer density (1.765 g/cm^3).

Morphology of PVDF Membranes. The surface and cross-section morphologies of PVDF membranes (dried at ambient temperature) were observed using scanning electron microscopy (SEM) (HITACHI, S-3400N). The samples were immersed in liquid nitrogen and fractured, and then sputtered with gold, and cross section and top surface configurations of samples were obtained.

Dynamic Contact Angle. A contact angle analyzer (JC2000D1, Shanghai Zhongchen Digital Technology Apparatus, China) was used to investigate dynamic contact angles (DCA) (θ) of PVDF membranes. A water droplet of 0.2 μL from a needle tip dispersed on the membranes surface. The machine was coupled with a camera enabling image capture at 10 frames/s. Contact angles were determined from these images with the specific calculation software. To ensure that the results were sufficiently credible, the experimental errors in measuring the θ values were evaluated to be less than $\pm 0.5°$. Measurement for each set of samples was performed in triplicate and the average data of contact angles were taken.

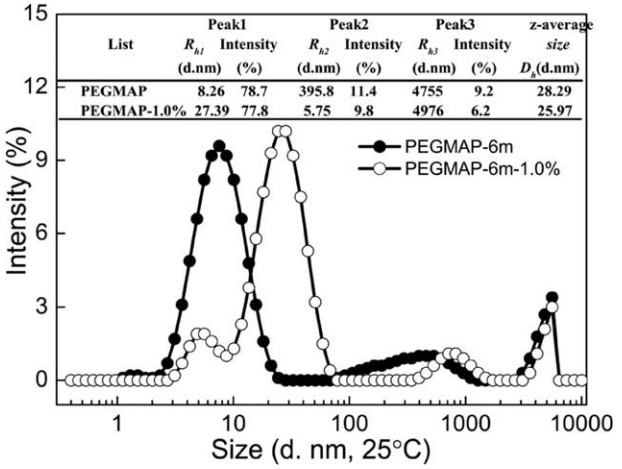

Figure 3. Intensity-weighted aggregate size distribution of various composition systems in selective cosolvents.

Mechanical Properties of PVDF Membranes. Mechanical properties were conducted using Microcomputer-Digital Display Integrative Control Testing Machine (QJ210A, Shanghai Qingji Instrument Sciences and Technology, China) at ambient temperature. The flat sample of settled width of 15 cm was clamped at both ends and pulled in tension at a constant elongation speed of 50 mm/min with an initial length of 25 cm. Break strength, elongation at break, and Young's modulus were obtained from the stress–strain curves through the average of at least five measurements.

RESULTS AND DISCUSSION

Determination of Basic Physical–Chemical Properties of Casting Solution

The intensity size and size distribution of submicron-sized particles, proteins, and reverse micelles can be probed accurately by DLS. DLS uses the scattered light to measure the rate of diffusion of the aggregated macromolecules in solution. Because of the sensibility of the equipment, only the dilute solution with a low polymer concentration can be measured. However, it is possible to provide the information about the morphology modulation of the PVDF dilute solution via polymerization.

Figure 3 shows the detail information for the intensity-weight of the supramolecular aggregates of the monomers and 1.0 wt % PVDF-monomers via polymerization in the selective cosolvent. The result reveals that the distribution of the supramolecular aggregates of the PEGMA and MMA monomers via polymerization is obviously narrow, and the domination aggregates are the micelles (size: 1–10 nm). This evidences the formation of the copolymer aggregates with small-size via polymerization.[44] After the addition of 1.0 wt % PVDF, it could be obtained that the R_h of the dominating population aggregates with narrow distribution enlarges. The supramolecular aggregates of the PVDF-copolymer contribute to the enlarged R_h of the PVDF-monomers system via polymerization, which suggests the microstructure adjustment of polymer solution and

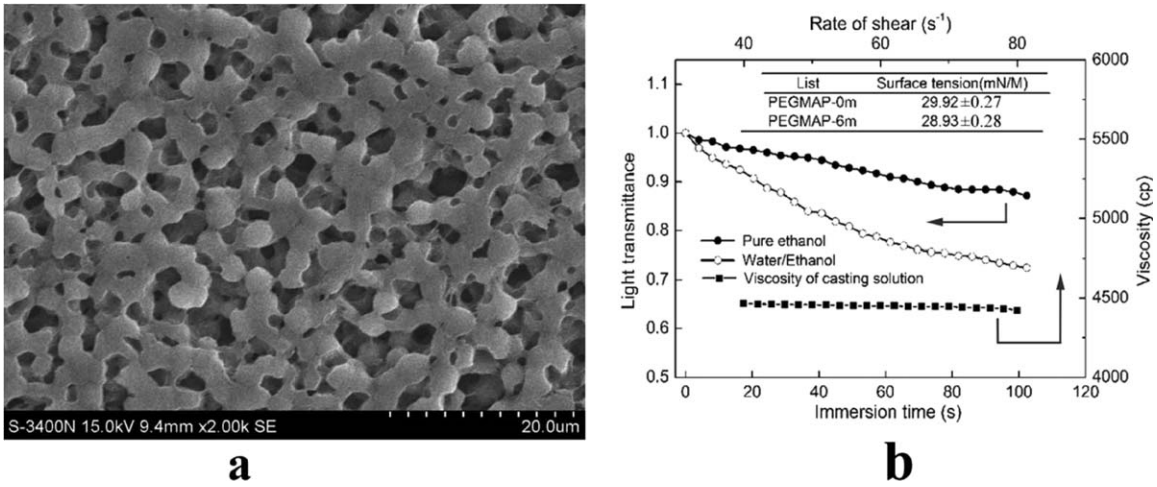

Figure 4. Morphology (a) and physical properties (b) of PVDF casting solution.

the conformation of PVDF. It was believed that the hydrophobic group of the copolymer contributed to either the adsorption of polymer over the copolymer layer or the formation of mixed adsorption layers.[45] The formation of the supramolecular aggregates of PVDF-copolymer with narrow distribution confirms the existence of the hydrophobic groups of the copolymer. The sharply decreased D_h of the 1.0 wt % PVDF-monomers system via free radical polymerization is attributed to the additional enhancement of the lowly coiled state and increased entanglement with the neighboring chains of PVDF, which is caused by the formation of the supramolecular aggregates of the PVDF-copolymer.

DLS was used to get the information about the morphology modulation of the PVDF dilute solution during polymerization. Then the conformation of 18.0 wt % PVDF is further evidenced by the morphology images of PVDF casting solution as shown in Figure 4(a). The images exhibit irregular mesh-like network of continuous domains, which in consistent with the DLS result of the formation of the supramolecular aggregates with narrow distribution.

The physical–chemical properties of PVDF casting solution including the precipitation kinetics, viscosity, and surface tension are presented in Figure 4(b). The precipitation curves of PVDF casting solution in water–ethanol and ethanol coagulants show delay demixing process, and the delay time in ethanol coagulant is longer than that of water–ethanol coagulant. The viscosity curve exhibits a shear-thinning behavior. The strong interconnection of the supramolecular aggregates of PVDF-copolymer enhances the chain entanglement degree of PVDF, and it determines the viscosities.[46] The novel observation is that the polymer solution via polymerization exhibits trivial strain thinning behavior. This implies that the strong molecular interconnection dominates the chain stretching and sliding under shear in these solution systems.[46] The surface tension of the various PVDF casting solutions without/via polymerization is presented in Figure 4(b). It shows that surface tension decreases after polymerization. It is the microstructure adjustment of the polymer solution that beneficial to the decreasing surface tension.

Table II. Filtration Properties of PVDF Membranes Prepared with Various Residence Times in the Two First Coagulants

Membrane list	J_W (L m^{-2} h^{-1} bar^{-1})	J_R (L m^{-2} h^{-1} bar^{-1})	E (%)
MWE-5	133 ± 2.2	55 ± 1.2	72.9
MWE-10	200 ± 2.5	85 ± 1.5	73.7
MWE-15	245 ± 1.4	115 ± 1.3	74.5
MWE-30	310 ± 1.3	155 ± 1.2	76.7
ME-5	915 ± 8.2	535 ± 5.4	75.9
ME-10	1550 ± 5.5	975 ± 4.2	79.7
ME-15	1680 ± 6.2	1200 ± 4.1	83.3
ME-30	2300 ± 9.7	1780 ± 7.2	86.8

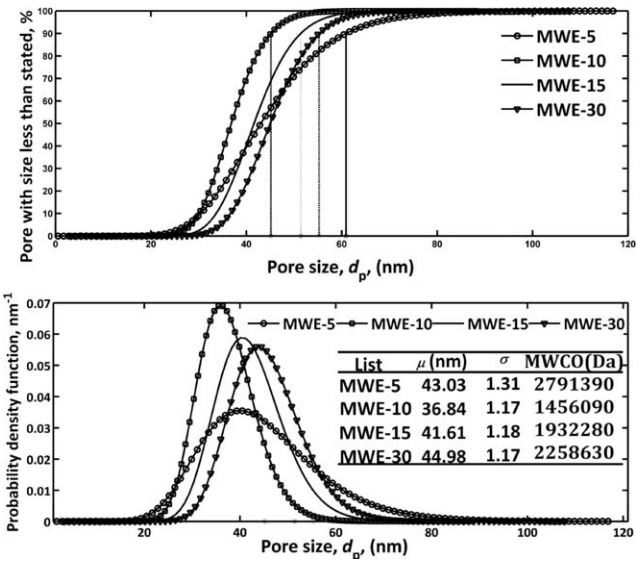

Figure 5. Cumulative pore size distribution curves and probability density function curves of various PVDF membranes prepared with various residence times from the water–ethanol first coagulant.

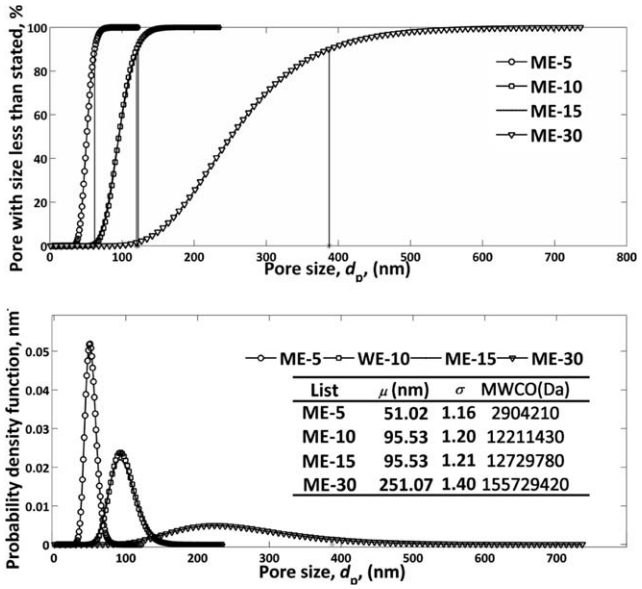

Figure 6. Cumulative pore size distribution curves and probability density function curves of various PVDF membranes prepared with various residence times from the ethanol first coagulant.

Filtration Properties of Resultant PVDF Performances

The relationship between the residence times and the filtration properties of resultant PVDF is shown in Table II. The results show that the pure water flux increases as increase of the residence time. Although the shorter time demixing process in water–ethanol coagulant limits the filtration improvement of PVDF membranes, the longer time demixing process in ethanol coagulant explains the enlarger flux.[16]

The cumulative pore size distributions and probability density function curves of PVDF membranes prepared from the two first coagulants are shown in Figures 5 and 6, respectively. Their corresponding μ, σ, and MWCO are also given in the two figures. Figure 5 exhibits that PVDF membranes prepared from water–ethanol first coagulant with various residence times possess narrow distribution pore size. When the residence time is 5 s, the μ is 43.03 nm, and the μ of the membranes with narrow distribution pore size significantly decreases as the residence time is 10 s. The novel result is that the μ increase as further increasing of the residence time, while the distribution of the pore size is constant narrow. The narrow distribution pore size is consistent with the supramolecular aggregates in the corresponding casting solution. This implies that the time for the pore-forming of those supramolecular aggregates is less than 5 s. The dominating demixing process of the casting solution in water–ethanol coagulant is 5–10 s.

As a soft coagulant, ethanol coagulant contributes to crystallization of the PVDF-TEP-DMAc-PEGMA-MMA system prior to liquid–liquid demixing.[37,41,47] It could be obviously observed from Figure 5 that the pore size distribution is narrow, with increasing μ and MWCO. The longer residence

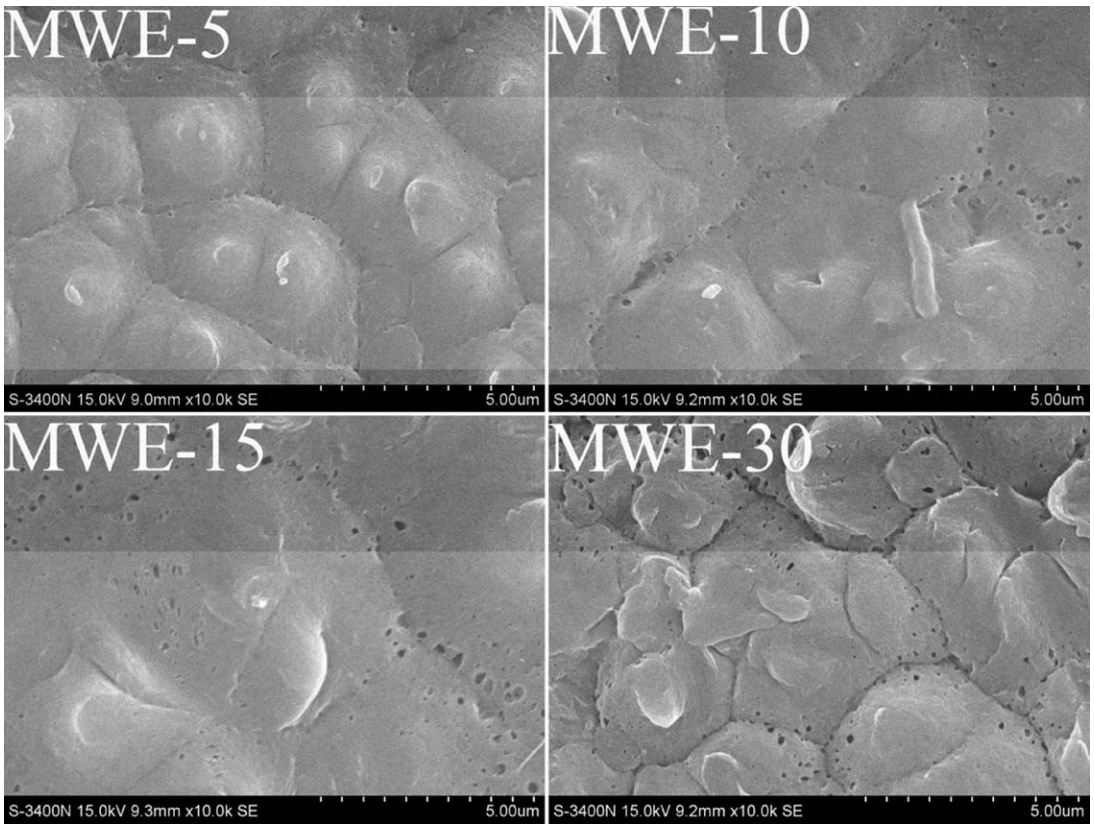

Figure 7. (a) SEM images of the top-surface of the PVDF membranes prepared with water–ethanol. (b) SEM images of the cross-section of the PVDF membranes prepared with water–ethanol.

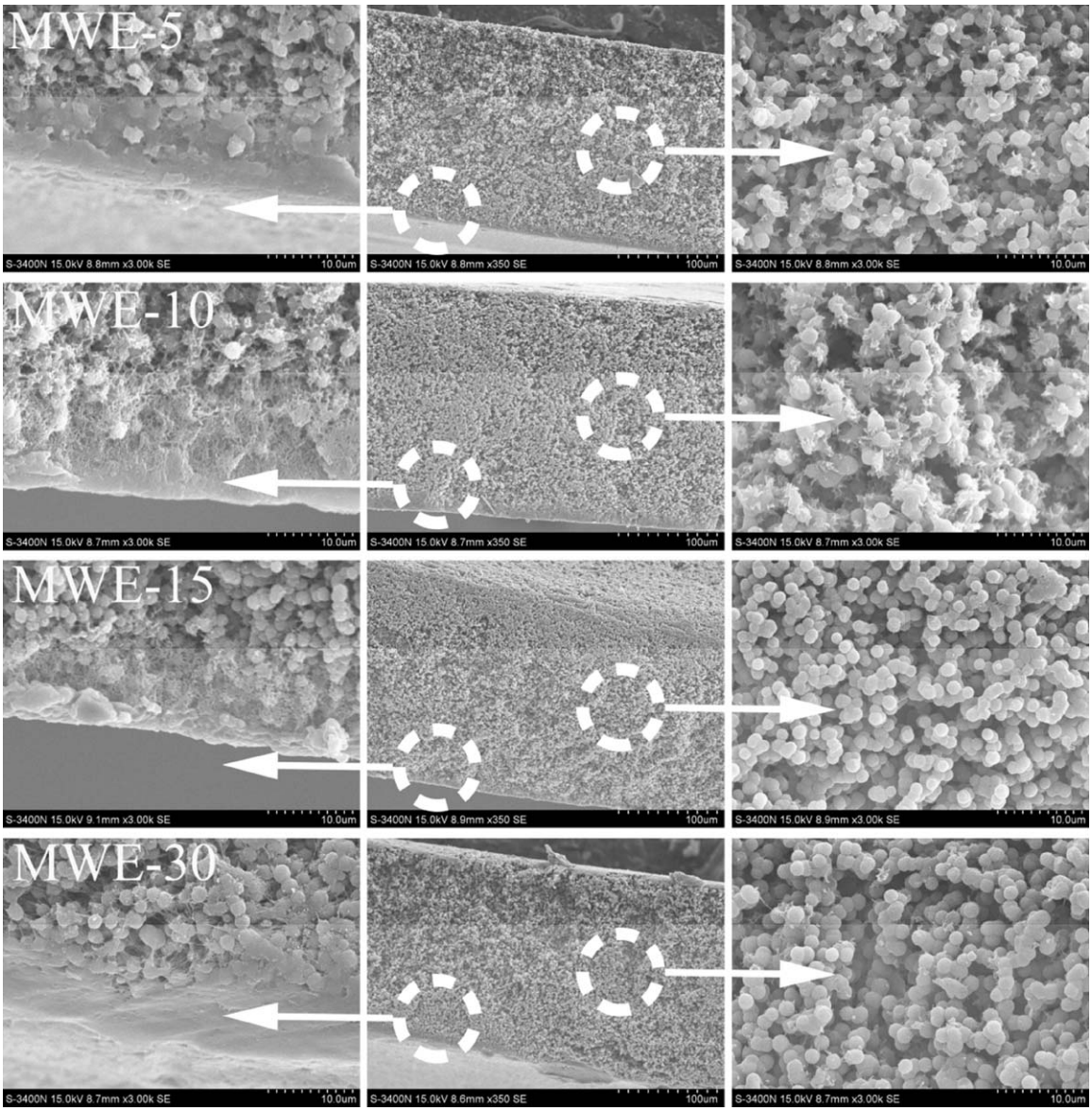

Figure 7. (Continued)

time is, the larger MWCO of resultant PVDF membranes are. A comparison of Figures 5 and 6 shows that the longer time delay demixing process in ethanol coagulant is beneficial to the increasing μ and MWCO. This is beneficial to the pore-forming of the copolymer. Apparently, Figure 6 reveals that the influence of 5 s residence time on the μ and MWCO of PVDF membranes is not obviously. The μ and MWCO of PVDF membranes prepared with residence times of 10 s and 15 s are close; the μ and MWCO significantly increase when the residence time is 30 s. This shows that the dominating demixing process in ethanol coagulant is 10–15 s. Combined with the flux data in Table II, it shows that the increasing μ is coincided with the increasing flux. Furthermore, the narrow distribution pore size is consistent with the narrow distribution supramolecular aggregates in the corresponding casting solution.

Morphologies and Mechanical Properties of the Resultant Membranes

The top surface and cross-section morphologies of PVDF membranes prepared with the various residence times in water–ethanol and ethanol coagulants as first coagulants are shown in Figures 7 and 8, respectively. High-magnification morphologies of the near skin layer and main bulk of the cross section were investigated to show the detail morphologies of the interior structure of PVDF membranes. All membranes show an asymmetric morphology of sponge-like structure in the sub-layer with the various skin layers.

Figure 7(a,b) reveals that various residence times in water–ethanol first coagulant result in a lotus-type appearance. The lotus becomes dense and wizened as residence time increasing. The typical agglomerates of the globules construct the interior of the PVDF bulk, whereas the globules are replaced by the regular

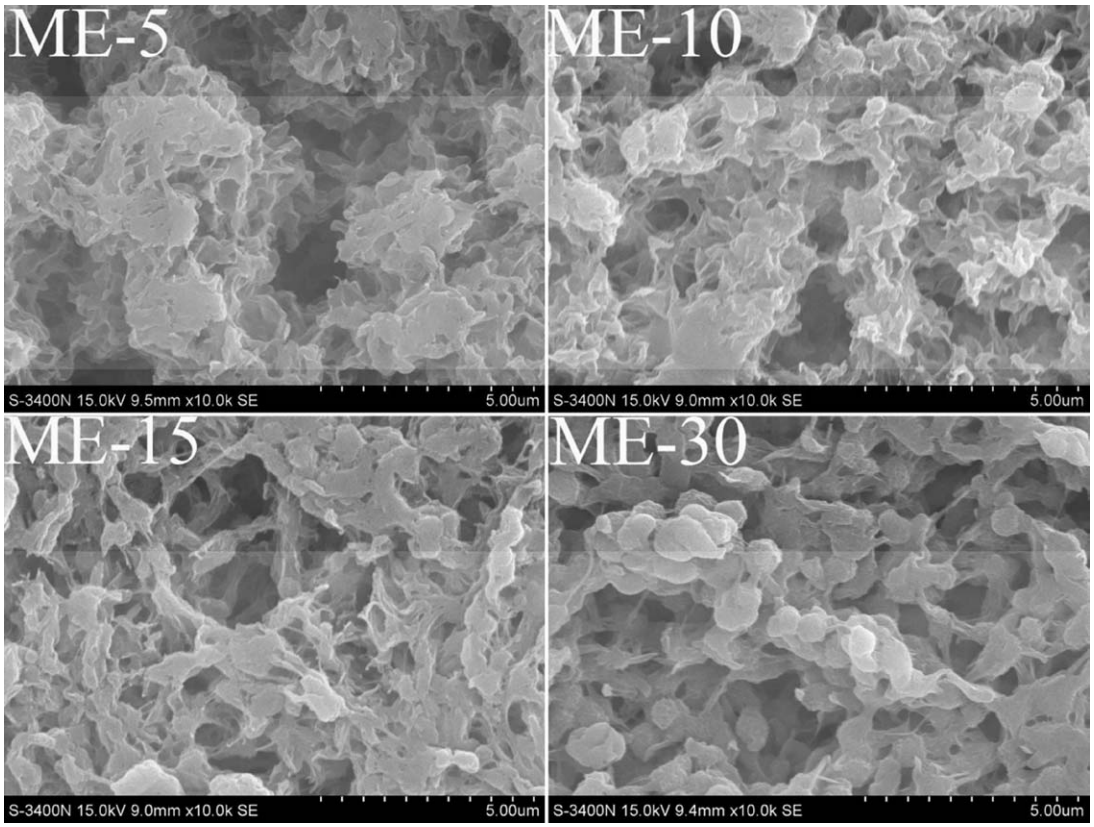

Figure 8. (a) SEM images of the top-surface of the PVDF membranes prepared with ethanol. (b) SEM images of the cross-section of the PVDF membranes prepared with ethanol.

inter-globules (with one of the globules bearing on the surface of another) in the case of the residence time increasing. Those inter-globules become loose packing with residence time increasing. Those inter-globules nanograins are consistent with the formation of the supramolecular aggregates with narrow distribution in the casting solution via polymerization. During the delay demixing process in the water–ethanol first coagulant with both liquid–liquid demixing and crystallization, the interconnection between PVDF and the copolymer provides an unbalance resistance to the surface-segregation of the polar head group of the copolymer, which contributes to the formation of cellular PVDF nanograins.[48] And the typical wrinkle configurations as SEM images shown explain the low flux of those PVDF membranes.

However, the morphologies of the PVDF membranes prepared from ethanol as first coagulant with various residence times display significant differences. Figure 8(a) shows that their top surface is skinless, and the nanograins regularly arranged. The formation of the porous structures, which is coincided with the increasing flux of those membranes.[16] As showed in Figure 8(b), the cross-sectional structure under high magnification shows the detail nanograins that constructed the membrane bulk, and three distinct regions could be identified. Near the top surface is the inter-globules. The skin layer near the bottom surface exhibits a cellular morphology. With residence time increase, the inter-globules shift to the cellular morphology. Ethanol coagulant contributes to crystallization of the polymer prior to liquid–liquid demixing. All the crystalline nanograins are nucleated and grown in a similar concentration field and finally fused together to form a bicontinuous structure.[48] Additionally, the confine of the supramolecular aggregates during the delay demixing process contributes to the formation of cellular PVDF nanograins.

Mechanical properties of the PVDF membranes in terms of break strength, elongation at break, and Young's modulus are shown in Table III. The mechanical properties decrease as residence time increase in the water–ethanol coagulant. The loose packing inter-globules that constructed the membranes bulk explain their poor mechanical properties. The break strength, elongation at break and Young's modulus of the membranes increases as residence time increasing in ethanol coagulants. The shift of the inter-globules to the cellular morphology probably contributes to the mechanical properties improvement.

Contact Angle Measurement

To investigate the change in hydrophilicity change of the top-surface and bottom-surface of the membranes prepared with the various residence times in as the two first coagulants, the dynamic contact angle data of all membranes are characterized by the curve of water drop angle to contact time as shown in Figure 9. The curves show that all membranes possess larger initial contact angle θ_S (or advancing contact angle) steady high equilibrium contact angle θ_E of membranes. The discrepancy in

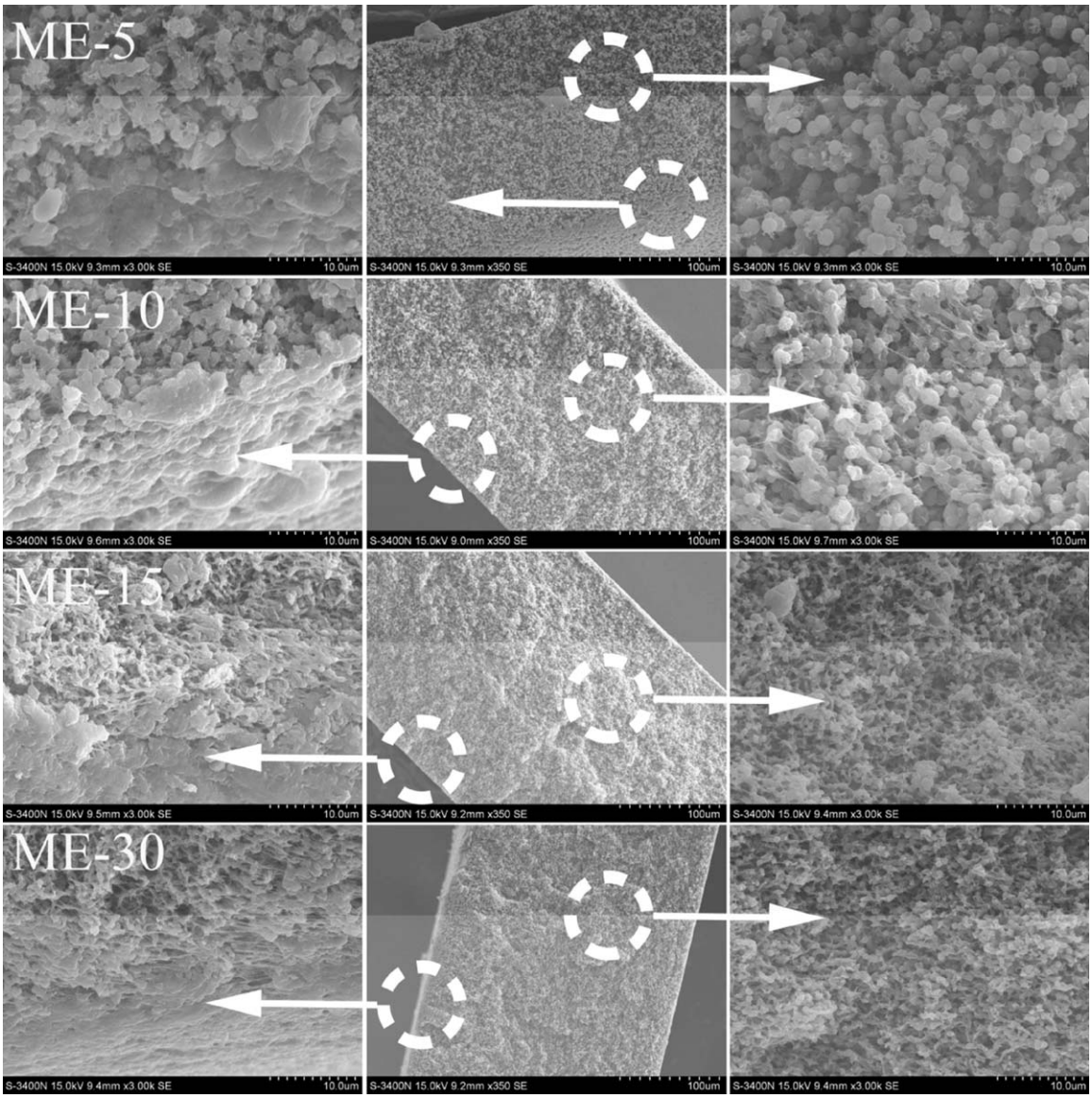

Figure 8. (Continued)

θ_S and θ_E of those membranes is not much with measurement time. It could be observed that the contact angle of both surfaces of PVDF membranes decreased with increase in residence time in the two coagulants, and the top-surface of membranes showed better hydrophilicity than that of the bottom surface. It is believed that the polar head groups of the copolymer have

Table III. Mechanical Properties of PVDF Membranes Prepared with Various Residence Times

Membrane list	Break strength (MPa)	Elongation ratio at break (%)	Young's modulus (MPa)
MWE-5	2.25 ± 0.21	78.78 ± 0.76	56.97 ± 0.35
MWE-10	2.05 ± 0.34	62.78 ± 0.53	52.65 ± 0.33
MWE-15	1.98 ± 0.29	60.85 ± 0.23	42.55 ± 0.41
MWE-30	1.72 ± 0.12	57.34 ± 0.34	39.84 ± 0.39
ME-5	1.23 ± 0.32	32.45 ± 0.22	30.62 ± 0.23
ME-10	1.93 ± 0.25	45.83 ± 0.22	38.68 ± 0.28
ME-15	2.95 ± 0.37	121.0 ± 0.57	72.17 ± 0.21
ME-30	3.34 ± 0.28	144.5 ± 0.76	77.26 ± 0.30

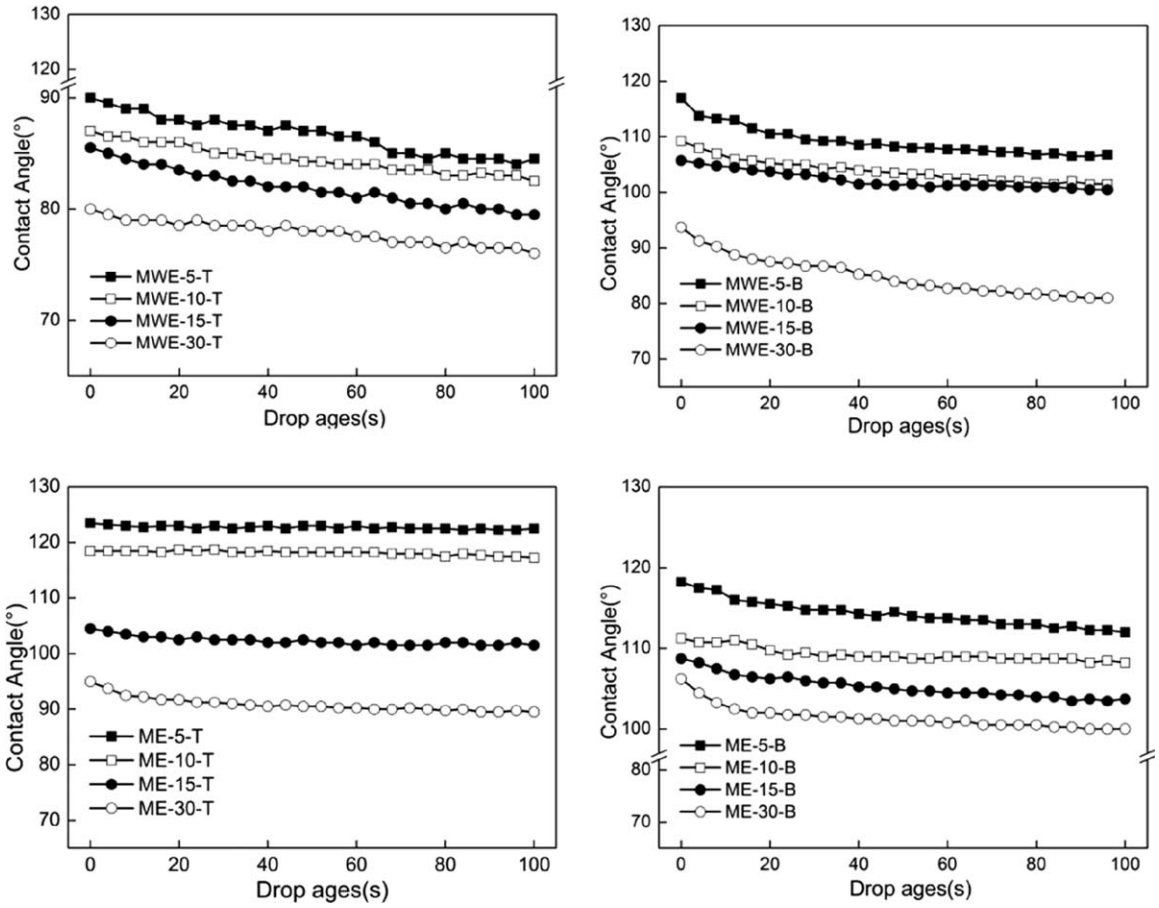

Figure 9. Dynamic contact angles of PVDF membranes prepared with various residence time in water–ethanol and ethanol coagulants (T: top-surface; B: bottom-surface).

self-segregated on the both surfaces of membranes, resulting in the decreasing θ_S and θ_E.[16]

CONCLUSION

PVDF membranes with better filtration properties, narrow distribution pore size, and enlarged recovery water flux were successfully synthesized with various residence times in water–ethanol and ethanol as first coagulants. All PVDF membranes prepared with longer residence time in the two coagulants possessed improved filtration properties and hydrophilicity. In comparison to shorter time demixing process, the longer time demixing process in the ethanol coagulant contributed to better filtration and hydrophilicity. Besides, the longer time demixing process in the ethanol coagulant contributed to better filtration and hydrophilicity. Additionally, the confine of the supramolecular aggregates during the delay demixing process was consisting with the narrow distribution μ and MWCO of the resultant PVDF membranes. The globules that constructed the membranes bulk prepared from water–ethanol coagulant were replaced by the regular inter-globules (with one of the globules bearing on the surface of another) in case of increased residence time. It explained decrease in mechanical properties of the corresponding PVDF membranes. While the longer time delayed demixing process in ethanol coagulant result in the shift of inter-globules to the cellular morphology, which was beneficial for mechanical properties improvement.

ACKNOWLEDGMENTS

The authors thank Key Technology R&D Program of Shanghai Committee of Science and Technology in China (11DZ1205201) for financial support by the National Natural Science Foundation of China (51172144) and Shanghai Union Program (LM201249).

REFERENCES

1. Rautenbach, R.; Vossenkaul, K.; Linn, T.; Katz, T. *Destlination* **1996**, *247*, 108.
2. Sun, C.; Leiknes, T.; Weitzenböckand, J.; Thorstensen, B. *Sep. Purif. Technol.* **2010**, *22*, 75.
3. Sagbo, O.; Sun, Y.; Haoand, A.; Gu, P. *Sep. Purif. Technol.* **2008**, *320*, 58.
4. Bangxiao, C. *Filtr. Sep.* **2005**, *33*, 42.
5. Daufin, G.; Escudier, J. P.; Carrère, H.; Bérot, S.; Fillaudeauand, L.; Decloux, M. *Food Bioprod. Process.* **2001**, *89*, 79.
6. Spyropoulosa, F.; Hancocksand, R. D.; Norton, I. T. *Procedia Food Sci.* **2011**, *920*, 1.

7. Katoh, R.; Asano, Y.; Furuya, A.; Sotoyamaand, K.; Tomita, M. *J. Membr. Sci.* **1996**, *131*, 113.
8. Charcosset, C. *J. Food Eng.* **2009**, *241*, 92.
9. Takht Ravanchi, M.; Kaghazchiand, T.; Kargari, A. *Desalination* **2009**, *199*, 235.
10. Madaeni, S. S.; Ahmadi Monfared, H.; Vatanpour, V.; Arabi Shamsabadi, A.; Salehi, E.; Daraei, P.; Lakiand, S.; Khatami, S. M. *Desalination* **2012**, *87*, 293.
11. Forsythea, J. S.; Hillb, D. J. T. *Progr. Polym. Sci.* **2000**, *101*, 25.
12. Wangand, P.; Chung, T.-S. *J. Membr. Sci.* **2012**, *361*, 421.
13. Sukitpaneenitand, P.; Chung, T.-S. *J. Membr. Sci.* **2009**, *192*, 340.
14. Ong, Y. K.; Widjojoand, N.; Chung, T.-S. *J. Membr. Sci.* **2011**, *149*, 378.
15. Zhang, M.; Zhang, A. Q.; Zhu, B. K.; Duand, C. H.; Xu, Y. Y. *J. Membr. Sci.* **2008**, *169*, 319.
16. Zhang, P. Y.; Yang, H.; Xu, Z. L.; Wei, Y. M.; Guoand, J. L.; Chen, D. G. *J. Polym. Res.* **2013**, *20*, 1.
17. Zhang, P. Y.; Yang, H.; Xu, Z. L. *Ind. Eng. Chem. Res.* **2012**, *4388*, 51.
18. Zhang, G.; Ji, S.; Gao, X.; Liu, Z. *J. Membr. Sci.* **2008**, *28*, 309.
19. Persson, K. M.; Trägdh, G.; Dejmek, P. *J. Membr. Sci.* **1993**, *51*, 76.
20. Wang, Y. N.; Tang, C. Y. *J. Membr. Sci.* **2011**, *275*, 376.
21. Yang, Q.; Xu, Z. K.; Dai, Z. W.; Wang, J. L.; Ulbricht, M. *Chem. Mater.* **2005**, *3050*, 17.
22. Zhao, Y.-H.; Qian, Y.-L.; Zhu, B.-K.; Xu, Y.-Y. *J. Membr. Sci.* **2008**, *567*, 310.
23. Rahimpour, A.; Madaeni, S. S.; Zereshki, S.; Mansourpanah, Y. *Appl. Surf. Sci.* **2009**, *7455*, 255.
24. Boributh, S.; Chanachaiand, A.; Jiraratananon, R. *J. Membr. Sci.* **2009**, *97*, 342.
25. Oh, S. J.; Kim, N.; Lee, Y. T. *J. Membr. Sci.* **2009**, *13*, 345.
26. Masuelli, M. A.; Grasselli, M.; Marchese, J.; Ochoa, N. A. *J. Membr. Sci.* **2012**, *91*, 389.
27. Sui, Y.; Wang, Z.; Gao, X.; Gao, C. *J. Membr. Sci.* **2012**, *38*, 413.
28. Zhang, P. Y.; Wang, Y. L.; Xu, Z. L.; Yang, H. *Desalination* **2011**, *186*, 278.
29. Lv, R.; Zhou, J.; Du, Q.; Wang, H.; Zhong, W. *J. Membr. Sci.* **2006**, *700*, 281.
30. Yoo, S. H.; Kim, J. H.; Jho, J. Y.; Won, J.; Kang, Y. S. *J. Membr. Sci.* **2004**, *203*, 236.
31. Simone, S.; Figoli, A.; Criscuoli, A.; Carnevale, M. C.; Rosselli, A.; Drioli, E. *J. Membr. Sci.* **2010**, *219*, 364.
32. Wongchitphimon, S.; Wang, R.; Jiraratananon, R.; Shi, L.; Loh, C. H. *J. Membr. Sci.* **2011**, *329*, 369.
33. Saljoughi, E.; Amirilarganiand, M.; Mohammadi, T. *Desalination* **2010**, *72*, 262.
34. Kimand, J. H.; Lee, K. H. *J. Membr. Sci.* **1998**, *153*, 138.
35. Chou, W. L.; Yu, D. G.; Yang, M. C.; Jou, C. H. *Sep. Purif. Technol.* **2007**, *209*, 57.
36. Ma, Y.; Shi, F.; Ma, J.; Wu, M.; Zhang, J.; Gao, C. *Desalination* **2011**, *51*, 272.
37. Alsalhy, Q. F.; Rashid, K. T.; Ibrahim, S. S.; Ghanim, A. H.; Van der Bruggen, B.; Luis, P.; Zablouk, M. *J. Appl. Polym. Sci.* **2013**, *3304*, 129.
38. Liu, F.; Xu, Y.; Zhu, B.; Zhang, F.; Zhu, L. *J. Membr. Sci.* **2009**, *331*, 345.
39. Hussain, H.; Tan, B. H.; Gudipati, C. S.; He, C. B.; Liu, Y.; Davis, T. P. *Langmuir* **2009**, *5557*, 25.
40. Hashim, N. A.; Liu, F.; Li, K. *J. Membr. Sci.* **2009**, *134*, 345.
41. Buonomenna, M. G.; Macchi, P.; Davoliand, M.; Drioli, E. *Eur. Polym. J.* **2007**, *1557*, 43.
42. Zhang, P.-Y.; Xu, Z.-L.; Yang, H.; Wei, Y.-M.; Wu, W.-Z.; Chen, D.-G. *Desalination* **2013**, *47*, 319.
43. Yang, Q.; Chung, T. S.; Santoso, Y. E. *J. Membr. Sci.* **2007**, *153*, 290.
44. Letchford, K.; Burt, H. *Eur. J. Pharm. Biopharm.* **2007**, *259*, 65.
45. Petkova, R.; Tcholakova, S.; Denkov, N. D. *Langmuir* **2012**, *4996*, 28.
46. Sukitpaneenit, P.; Chung, T. S. *J. Membr. Sci.* **2009**, *192*, 340.
47. Peng, B.; Li, Y.; Zhao, Z.; Chen, Y.; Han, C. C. *J. Appl. Polym. Sci.* **2013**, n/a.
48. Young, T. H.; Cheng, L. P.; Lin, D. J.; Fane, L.; Chuang, W. Y. *Polymer* **1999**, *5315*, 40.